Large positive magnetoresistance and transport properties of intercalated Cu oxides

1998 J. Phys.: Condens. Matter 10 4685

(http://iopscience.iop.org/0953-8984/10/21/023)

J. Phys.: Condens. Matter **10** (1998) 4685–4698. Printed in the UK PII: S0953-8984(98)83868-X

Large positive magnetoresistance and transport properties of intercalated Cu oxides

L Grigoryan†, M Furusawa‡, H Hori‡ and M Tokumoto§

† Department of Physics, University of Kentucky, Lexington, KY 40506, USA
‡ JAIST, Hokuriku, Ishikawa 923, Japan
§ ETL, 1-1-4 Umezono, Tsukuba, Ibaraki 305, Japan

Received 28 April 1997, in final form 21 January 1998

Abstract. Magnetism and electrical resistance as a function of magnetic field, temperature and chemical composition are studied in Cu oxides intercalated with metal phthalocyanines MPc, where M is Fe or Ni, and Pc is $C_{32}H_{16}N_8$. An unusually large positive magnetoresistance (MR) ~1200% is observed in FePc-intercalated $Bi_2Sr_2Ca_{n-1}Cu_nO_{2n+4}$ samples with $n = 2$. The magnitude of MR dropped to 40% and ~0% in the FePc-intercalated $n = 3$ and $n = 4$ samples, respectively, and to ~300% in the NiPc-intercalated $n = 2$ sample. The possible mechanism responsible for the observed large MR is tentatively discussed in terms of a competition between the resonant spin-fluctuation and the spin-glass-like states.

1. Introduction

An unusually large magnetoresistance defined as $\mathrm{MR} = R(H) - R(0)/r(0)$, where R is the sample's resistance and H external magnetic field, was observed recently in metallic multilayer films and Mn-based oxides with perovskite crystal structure (see [1] for a recent review). Physical mechanisms, as well as typical values of large MR in multilayers and in Mn oxides are believed to be different, and the phenomenon is called either GMR (giant magnetoresistance) or CMR (colossal magnetoresistance), when referring to multilayers or Mn oxides, respectively. Both GMR and CMR are attracting great attention due to interesting basic physics as well as the highly promising technological applications, e.g., in magnetic recording.

In this work, we report the first observation of large MR of the order of 1200% in a new system, that is the intercalated high-T_c Cu oxides. The effects of chemical composition, as well as temperature and magnetic field on dc magnetization and dc resistance are investigated and discussed. In contrast to most multilayer and Mn oxide samples, where with application of a magnetic field the resistivity *decreases* (negative MR), in our system the resistivity *increases* (positive MR). The mechanism of the anomalous large MR in our samples is not well understood at this stage, and we will refer to it as LMR (meaning simply 'large MR'), to distinguish it from both GMR and CMR phenomena. Another important feature of our system is that it is created through intercalation (diffusion) of magnetic layers between the electrically conducting non-magnetic layers of the host Cu oxide crystal. We believe that this work may open up a new approach to creating LMR materials by using the intercalation method.

High-temperature superconducting Cu oxides have a layered crystal structure and some of them, such as BiSCCO ($Bi_2Sr_2Ca_{n-1}Cu_nO_{2n+4}$, where $n = 1$, 2 or 3 is the number of

0953-8984/98/214685+14$19.50

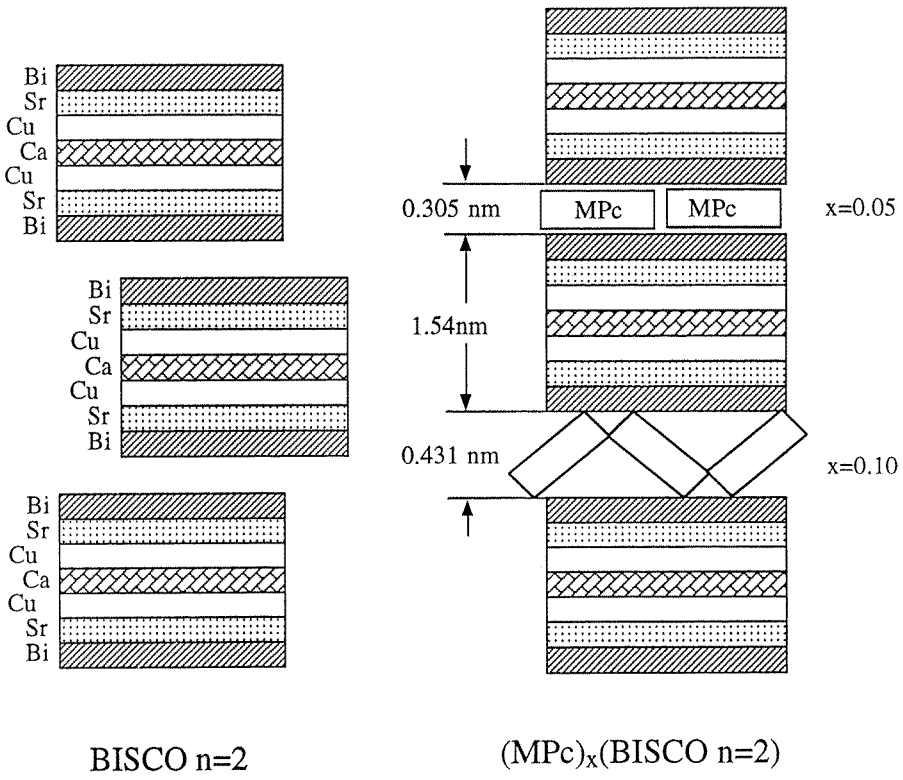

Figure 1. Scheme of the layered crystal structure in pristine BiSCCO $n = 2$ and two MPc-intercalated phases: $x = 0.05$ (the upper part) and $x = 0.10$ (the lower part).

Cu–O layers in the unit cell) can be intercalated with various atomic and molecular species bringing about a dramatic modification of the superconducting and normal-state properties [2–6]. In particular, intercalation of the BiSCCO $n = 2$ with metal phthalocyanines, MPc (where M is Fe or Ni, and Pc is $C_{32}H_{16}N_8$) has been shown to give rise to two new crystal structures with the ***c***-axis expanded by 0.305 or 0.431 nm in $(MPc)_x$ BiSCCO with $x = 0.05$ or 0.1, respectively [4] (figure 1). A combination of x-ray powder diffraction, scanning tunnelling microscopy and spectroscopy (STM/STS), optical absorption and reflection, FT infrared (IR) and far IR, micro-Raman scattering and electron spin resonance (ESR) data has indicated that MPc molecules were inserted between the double Bi–O layers, forming organic monolayers separating the unit cell blocks of the host oxide [4–7]. MPc molecules were not ordered within the intercalated layer. According to the STM/STS data, the intercalated MPc layers were electrically insulating, but they have been shown to play a crucial role in determining magnetic properties of the intercalated samples. In particular, measurements of dc magnetization and microwave absorption as a function of temperature and applied magnetic field indicated strong interaction between the magnetic ions at the intercalated MPc molecules, resulting in formation of spin-glass-like phases [4, 7].

Hence, using intercalation, one can create crystal structures where electrically conducting layers (such as Cu–O layers) are alternating with magnetic layers (such as FePc molecular layers). Electron transport along the ***c***-axis will be strongly dependent on scattering of conduction electrons in the MPc layers which, in its turn, depends on the sign and magnitude of both intra- and interlayer exchange between transition metal ions contained

in the intercalated MPc molecules. The exchange interaction is a complex function of concentration, intra-layer geometry and the particular type of magnetic ion in MPc and distance between the intercalated MPc layers, as well as the electronic structure of the host Cu oxide. In this work, we attempted to study the effect of varying some of these factors (e.g., particular M in MPc, number of layers in the unit cell of host Cu oxides) on magnetic and electrical properties of the samples.

2. Sample preparation and experimental details

The BiSCCO $n = 2$, $n = 3$ and $CuBa_2Ca_3Cu_4O_{10.5}$ ($n = 4$) samples with $T_c \sim 94$, 108 and 115 K, respectively, were prepared by the standard solid-state reaction. Resistivities of the pristine samples varied between ~0.1 and ~1 (mΩ cm) at room temperature and linearly decreased with cooling down to their respectively T_c. A BiSCCO $n = 2$ powder was exposed to vapours of FePc at 820 K in a 10^{-3} Torr vacuum for several days to produce intercalated $(FePc)_x$ (BiSCCO $n = 2$) sample. The fact of intercalation could be established from the x-ray powder diffraction (figure 2), elemental analysis and weight uptake data (see [4] for the details). The x-ray diffraction patterns of the intercalated pressed pellets indicate that the desired $x = 0.1$ ($c = 1.971$ nm) phase was formed only within an ~10 μm layer of the surface, while the interior part was comprised predominantly of the non-magnetic insulating $x = 0.05$ ($c = 1.845$ nm) phase. The energy dispersive x-ray spectroscopy (Hitachi) results indicated a fairly homogeneous distribution of Fe, Bi, Sr, Ca and Cu over the surface of the pellets. A steep drop in Fe content from $x = 0.1$ to 0.05 was observed when going from the ~10 μm surface layer into the bulk. To obtain a pure $x = 0.1$ phase for magnetic studies, a finely ground powder of BiSCCO $n = 2$ with grain size below ~10 μm was used for the intercalation. The same treatment procedure as described above was used to produce MPc-intercalated BiSCCO $n = 3$ and $CuBa_2Ca_3Cu_4O_{10.5}$ samples with three and four Cu–O layers in the unit cell, respectively. A simple heat treatment of the pristine BiSCCO $n = 2$ sample under the same conditions, but without the presence of any MPc, resulted only in a slight decrease of T_c, without any significant changes in XRD, magnetic or electrical properties.

The commercially (Aldrich) available samples of MPc (M = Fe, Ni, Pb or H_2) used for intercalation were purified by vacuum sublimation before use. The mixed-metal $(Fe_xM_{1-x})Pc$ samples were prepared by vacuum co-sublimation of corresponding amounts of purified FePc and MPc.

Measurements of dc magnetization were carried out with a Quantum Design SQUID magnetometer. Dc resistance (R) of the samples was measured by attaching four probes, arranged linearly at equal distances from each other to the surface of a pressed pellet bar, with a silver paste (the geometry is shown in the inset to figure 5). Resistivity (ρ) values were calculated as $\rho = (\pi t/\ln 2)R$, where t is the thickness of the conducting surface layer. The longitudinal MR was measured using the same four-probe arrangement and a superconducting 12 T magnet. The measurements taken with the reversed polarity of the magnets have shown that the response was symmetrical with respect to the direction of the external magnetic field.

3. Results and discussion

3.1. Magnetic properties

Before intercalation, the superconducting BiSCCO $n = 2$ samples exhibited weak, almost temperature-independent paramagnetism in the normal state. The superconductivity was

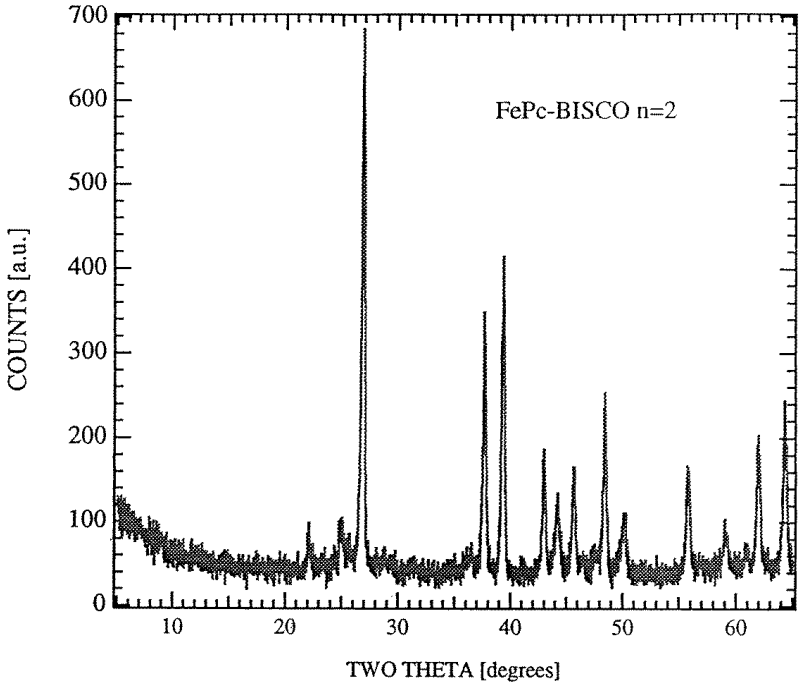

Figure 2. X-ray power diffraction in the $(FePc)_{0.10}$ (BiSCCO $n = 2$) sample. The diffraction pattern is similar to the one identified in [4].

totally suppressed upon the intercalation, but instead, the $(FePc)_{0.1}$ (BiSCCO $n = 2$) samples exhibited novel magnetic properties featuring complex magnetization–external field and temperature curves (figures 3 and 4). A sharp drop of the zero-field-cooled (ZFC) magnetization and concomitant increase of a divergence between the ZFC and the field-cooled (FC) magnetizations were observed at $T_0 \sim 130$ K (figure 3). The magnetization–field curves exhibited a non-linear, saturating behaviour in fields $H \sim 0.5$ T, with saturation magnetization $\sim$0.5 emu g^{-1} (figure 4). The magnetization–H curves retained a non-linear character up to about 750 K, and became linear upon further heating, indicating transition to a paramagnetic state.

Comparison of the magnetization–T, H curves measured below and above the T_0 indicated that the magnetic properties were different below the transition temperature (figures 3 and 4). In particular, the magnetization–H curves taken at 140 and 100 K looked almost identical to the ones taken at 280 and 10 K, respectively, clearly indicating that the sharp increase in both remanent magnetization and coercivity occurred around $T_0 \sim 130$ K. At the same time, the FC values of magnetization became strongly dependent on thermomagnetic history of the sample below the T_0. It is interesting to note that the transition temperature almost did not depend on the value of the applied magnetic field: it shifted from $\sim$130 down to $\sim$125 K when the applied field was increased from 10^{-3} to 1 T.

The transition temperature T_0 was virtually the same $\sim$130 K for the FePc-intercalated $n = 2$, $n = 3$ (figure 3) and $n = 4$ samples, as well as in the BiSCCO $n = 2$ and $n = 3$ samples intercalated with mixed MPc (such as $Ni_{1/3}Fe_{2/3}Pc$, $Cu_{1/2}Fe_{1/2}Pc$ or $Pb_{1/4}Fe_{3/4}Pc$). However, the transition could not be observed in either of the purely NiPc-, PbPc- or CuPc-intercalated (that is, not containing any significant amount of FePc) BiSCCO samples.

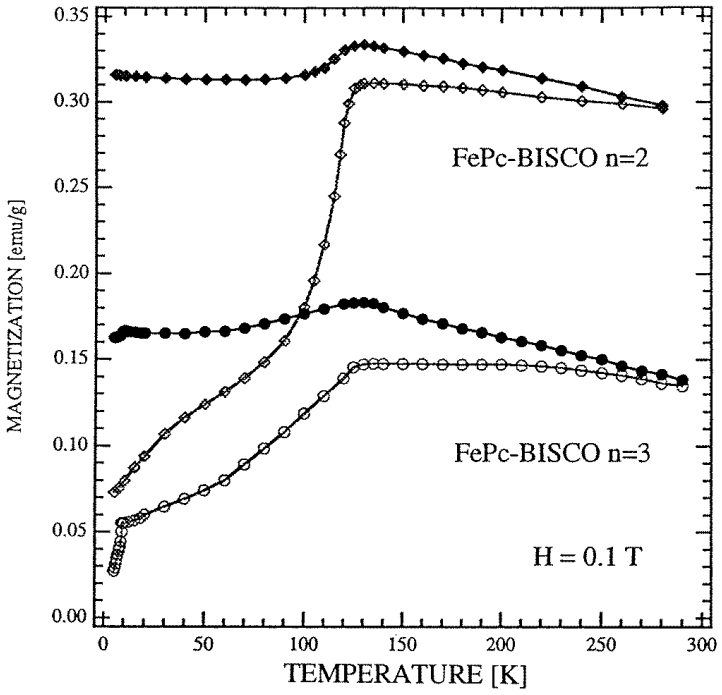

Figure 3. Magnetization–temperature curves in external magnetic field of 0.1 T for the FePc-intercalated BiSCCO $n = 2$ (diamonds) and $n = 3$ (circles) samples. Open and closed symbols refer to ZFC and FC values of magnetization, respectively.

The combination of the above experimental data, i.e., the decreased ZFC magnetization, thermomagnetic history-dependent FC magnetization and sharply increased irreversibilities, is a strong indication of a spin-glass-like behaviour in the vicinity of the spin-glass freezing temperature, $T_0 \sim 130$ K [8]. At very high temperatures a spin-glass system exhibits linear magnetization–H curves similar to those of a paramagnet, as the localized spins essentially do not interact. At lower temperatures, spin clusters are formed due to short-range dynamic spin–spin correlations. The coupling within and between the clusters is determined by the particular spatial spin distribution according to the so-called RKKY (Ruderman–Kittel–Kasuya–Yoshida) interaction among the localized spins mediated by the conduction electrons. At these temperatures the system may exhibit non-linear, saturating magnetization–H curves similar to those of a ferromagnet, but with very little or no hysteresis. With further cooling, size and density of clusters grow, eventually forming an 'infinite' glassy cluster of frozen spins below the freezing point. At low temperature $T < T_0$, a spin-glass is characterized by decreased magnetization at low fields, dependence of FC magnetization on thermo-magnetic history, sharply increased remanence and coercivity.

A spin-glass system is typically formed in a non-magnetic metal containing randomly distributed magnetic impurities (such as transition metals) in the range from 0.1 to 10% [8]. This criterion is readily applicable in our case, since the intercalated samples can be considered as ∼1% Fe ions randomly dispersed in metallic BiSCCO host. All the above features characteristic for a spin-glass behaviour at various temperature ranges were

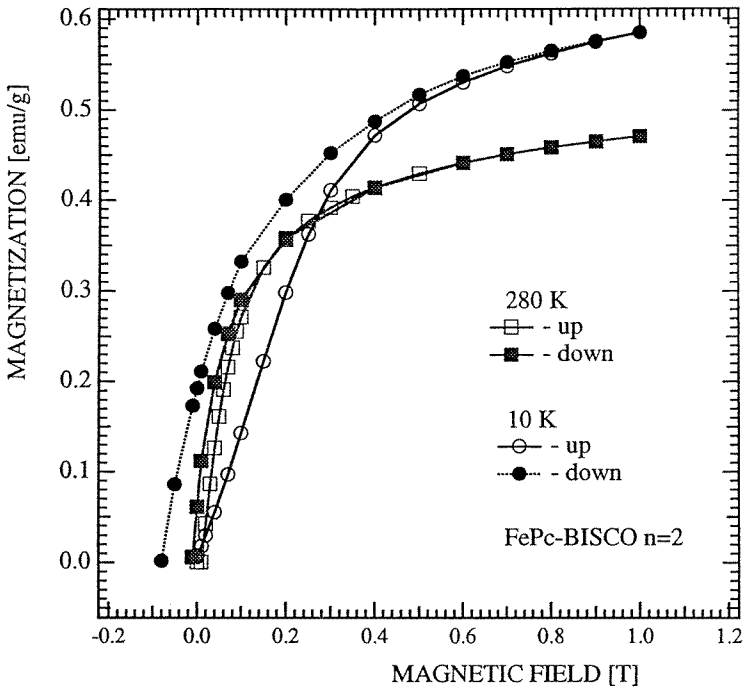

Figure 4. Magnetization–applied magnetic field curves at 280 (squares) and 10 K (circles) for the FePc-intercalated BiSCCO $n = 2$ sample. Open and closed symbols refer to values measured with increasing and decreasing field, respectively.

experimentally observed in our samples, thereby supporting our interpretation based on a spin-glass model. The fact that the transition can be observed only in the sample containing FePc relates its origin to the Fe ions at intercalated FePc molecules. It is also important to note that T_0 is virtually the same ($\sim$130 K) in the BiSCCO samples with different numbers of Cu–O layers, suggesting that T_0 is insensitive to the distance between the intercalated FePc layers. These data strongly suggest that the *intra*-layer exchange interactions between the intercalated FePc are the main factor responsible for the observed magnetic properties.

3.2. Electrical resistivity

In contrast to the magnetism, the dc resistivity appeared to be very much dependent on the host system (figures 5 and 6). For the $n = 3$ and $n = 4$ hosts, ρ decreased with cooling in a nearly linear fashion, similar to the normal-state ρ–T curves of the non-intercalated superconducting high-T_c oxides (figure 6). The specific type of intercalated MPc had very little if any effect on the ρ–T curves of the $n = 3$ and 4 samples. However, for the intercalated BiSCCO $n = 2$ system, ρ generally had a tendency to increase with cooling, and the ρ–T curves exhibited a complicated shape depending on the type of intercalated MPc. In particular, ρ in the FePc intercalate slightly decreased upon cooling from 300 down to 200 K, as well as below 40 K, in contrast to the monotonically increasing ρ in the NiPc intercalate (figure 5).

The $\rho(T)$ functional dependence in the intercalated BiSCCO $n = 2$ samples closely

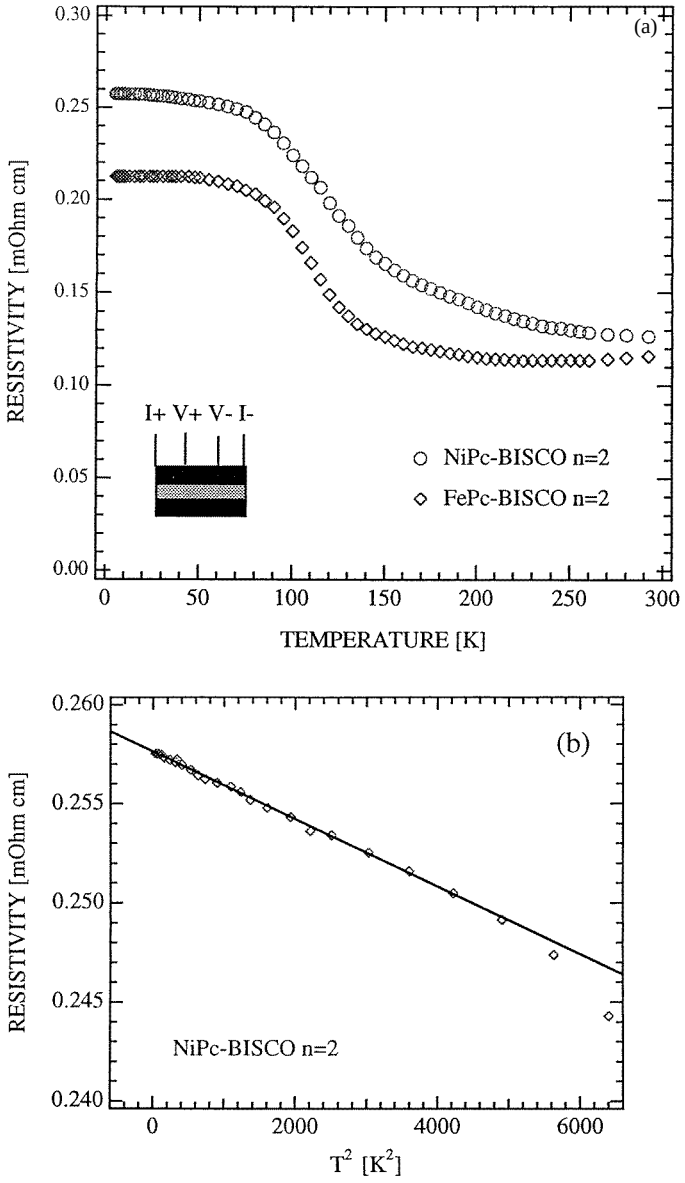

Figure 5. (a) Resistivity–temperature curves for the NiPc- (circles) and the FePc-intercalated (diamonds) BiSCCO $n = 2$ samples. The inset shows the geometry of four electrical probes on the surface of a mixed-phase pressed pellet. The filled and the shaded areas represent $x = 0.10$ and $x = 0.05$ phases, respectively. (b) Low-temperature resistivity in the NiPc-intercalated BiSCCO $n = 2$ sample plotted against T^2.

resembles the theoretical universal behaviour predicted for a non-magnetic metal with a transition metal impurity [9]. It is assumed that the impurity introduces a virtual bound state described by the Anderson model [10], and the resistivity is mainly determined by the scattering of conduction electrons by localized spin fluctuations [9]. At low temperatures

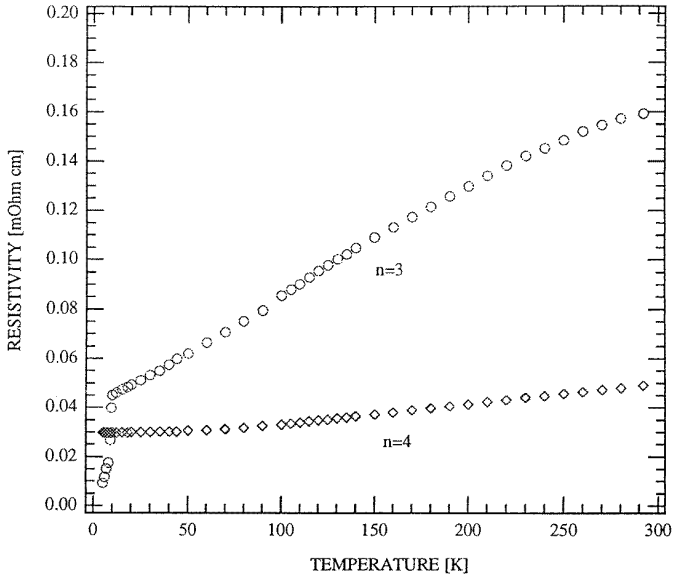

(a)

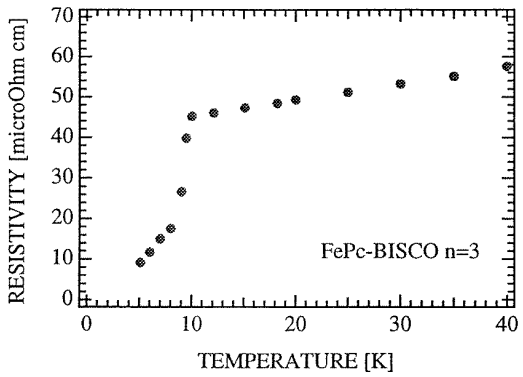

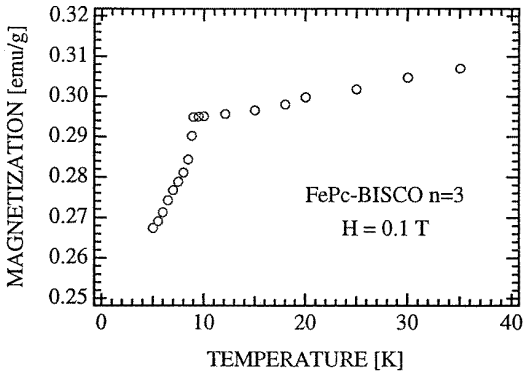

(b)

Figure 6. (a) Resistivity–temperature curves for the FePc-intercalated BiSCCO $n = 3$ (circles) and $n = 4$ (diamonds) samples. (b) The superconducting transition at $T_c \sim 9.5$ K in the FePc-intercalated BiSCCO $n = 3$ sample.

($T \ll T_{sf}$), a parabolic $R(T)$ dependence is predicted (including thermal broadening):

$$\rho(T) = \rho_0\left[1 - \left(\frac{T}{\Theta}\right)^2\right] \tag{1}$$

where

$$\Theta = \frac{2T_{sf}}{\pi U N_d(E_F)}. \tag{2}$$

Here U is the Coulomb repulsion between 3d electrons of opposite spin, $N_d(E_F)$ is the density of states at the Fermi level and T_{sf} is a characteristic spin-fluctuation temperature. With the temperature approaching T_{sf}, the parabolic $\rho(T)$ dependence is replaced with a linear relationship:

$$\rho \propto \left(1 - \frac{T}{2\Theta}\right). \tag{3}$$

At temperatures above T_{sf}, a logarithmic dependence characteristic of magnetic impurities is expected:

$$\rho \propto -\ln T. \tag{4}$$

Finally, at high temperatures ($T \gg T_{sf}$), resistivity decreases as inverse temperature:

$$\rho \propto \frac{1}{T}. \tag{5}$$

It is important to remember that this analysis applies to systems described by the Anderson model. However, in the case of the exchange-enhanced solids which are better described by the Wolff model [11], a similar analysis yields a universal curve which qualitatively is a mirror image of the one discussed above [12]. It should be noted that the natures of the spin fluctuations are the same in both models, and the sign of $\mathrm{d}\rho/\mathrm{d}T$ is determined by the condition of orthogonality between the host conduction states and the impurity 3d orbitals [13]. For the orthogonal states, $\mathrm{d}\rho/\mathrm{d}T < 0$ (Anderson model), while for the non-orthogonal ones, $\mathrm{d}\rho/\mathrm{d}T > 0$ (Wolff model) [13].

Application of these models to our samples shows that the ρ–T curves of the intercalated $n = 2$ system exhibiting $\mathrm{d}\rho/\mathrm{d}T < 0$ are in fairly good agreement with the predictions for the Anderson model (figure 5). In particular, the NiPc-intercalated $n = 2$ sample exhibits all the predicted regimes: parabolic at $T < 70$ K (figure 5(b)), linear at $80 < T < 130$ K, logarithmic at $140 < T < 200$ K and inverse T at $210 < T < 250$ K. A least-squares fit to the experimental data at $T < 130$ K according to (1)–(3) yields $\Theta \sim 270$ K, and $T_{sf} \sim 135$ K, assuming $\pi U N_d(E_F) = 1$. This estimate of T_{sf} is somewhat arbitrary as we have no data at this stage to show how correct the $\pi U N_d(E_F) = 1$ approximation is. However, it gives some idea of the order of magnitude for T_{sf}, namely, that $T_{sf} \sim T_0$.

The picture is somewhat more complicated in the FePc-intercalated $n = 2$ sample, where $\mathrm{d}\rho/\mathrm{d}T$ is very slightly positive at both $T < 40$ K and $T > 200$ K regions (figure 5). This deviation from the spin-fluctuation behaviour characteristic of isolated magnetic impurities may be due to additional contribution from either enhanced interaction between the Fe ions as compared to the Ni ions, or stronger phonon scattering. Both these contributions might lead to deviation from a pure spin-fluctuation behaviour manifested as an upturn of ρ ($\mathrm{d}\rho/\mathrm{d}T > 0$) at high temperatures. Another powerful competitor for the spin-fluctuation behaviour is the RKKY interaction characterized by the spin-freezing temperature, $T_0 \sim 130$ K in the FePc-intercalated samples. The resonant spin-fluctuation state may be quenched by the RKKY interaction, resulting in deviations from spin-fluctuation behaviour. In particular, this mechanism could be responsible for the positive

$d\rho/dT$ observed at low temperatures $T < 40$ K (figure 5). On the other hand, both $n = 3$ and $n = 4$ systems, independent of particular intercalated MPc, exhibit $d\rho/dT > 0$ in the whole temperature range from 300 down to 5 K, and in that sense their behaviour is (at least qualitatively) rather consistent with the Wolff model.

At this stage, it is difficult to explain why exactly the $n = 2$ intercalates are better described by the Anderson model, and the $n = 3$ and $n = 4$ ones by the Wolff model. One can speculate that the increasing number of Cu–O planes in the unit cell causes the Fermi level of the host oxide to shift, while the 3d orbitals of the intercalated MPc molecules remain the same independent of the host. In that case, the transition from the Anderson to the Wolff model may be related to the shift of the Fermi level with respect to the 3d orbitals, when going from the $n = 2$ to the $n = 3$ and the $n = 4$ systems. This kind of transition between the models, involving a sign change for $d\rho/dT$ as a function of position of the Fermi level with respect to the magnetic impurity level, was predicted theoretically in [14].

Finally, it is interesting to note that both the dc magnetization and resistance curves revealed a superconducting transition in both the FePc- and the NiPc-intercalated BiSCCO $n = 3$ (figure 6(b)). The onset transition temperature was ∼9.5 K and the ρ–T curves, in general, were also almost identical for both samples, indicating that the particular metal in intercalated MPc had little effect on resistivity. Similarly, the ρ–T curves were not notably different in the FePc- and NiPc-intercalated $n = 4$ samples, in contrast to the $n = 2$ system. However, only the $n = 3$ system MPc-intercalated samples have been found so far to exhibit superconductivity. The fact of the co-existence of superconductivity with a relatively large MR in the FePc-intercalated BiSCCO $n = 3$ system is intriguing, even though at this stage it is not clear whether these two phenomena are related.

3.3. Magnetoresistance

Very large positive values of MR > 1200% were obtained at ∼130 K in the FePc-intercalated BiSCCO $n = 2$ samples (figure 7(a)). These MR values exceed those obtained typically in GMR multilayer films [15, 16] and are rather comparable to the CMR values observed in Mn oxides [17–20]. In terms of a crystal structure, our system is also different from multilayers, but close to a Mn oxides. It should be noted, however, that in both above systems MR is usually negative, that is resistance *decreases* with applied field, in contrast to our samples, where *R increases* with applied field. The MR–T curves exhibit a distinct peak around the spin-glass freezing temperature, $T_0 \sim 130$ K (figure 7(b)) determined from dc magnetization measurements (figure 3). This is a strong indication that the anomalous large MR exhibited by our samples may be related to the magnetic transition. Similarly, in the case of Mn oxides, the CMR was observed to peak near the ferro- to paramagnetic transition temperature [17–20].

The magnitude of MR was found to be very sensitive to the host oxide; in particular, it dropped to ∼40% in the FePc-intercalated $n = 3$ (figure 8(a)) and ∼0% $n = 4$ (figure 8(b)) samples. We have also found that the values of MR decreased significantly if FePc (as an intercalant) was replaced, either partially or completely, with other MPc, such as NiPc, CuPc, H_2Pc or PbPc. In particular, the MR values for the BiSCCO $n = 2$ system dropped down to 850% and 300% in the cases of mixed-metal $Ni_{1/3}Fe_{2/3}Pc$ (prepared by a co-sublimation of one part NiPc and two parts FePc, figure 7(b)) and pure NiPc, respectively. This result correlates with the decreased saturation magnetization values, measured at 10 K, in the NiPc-containing samples (∼0.30 and ∼0.03 emu g^{-1}, respectively). The MR (as well as the saturation magnetization) values dropped virtually down to zero in the cases if

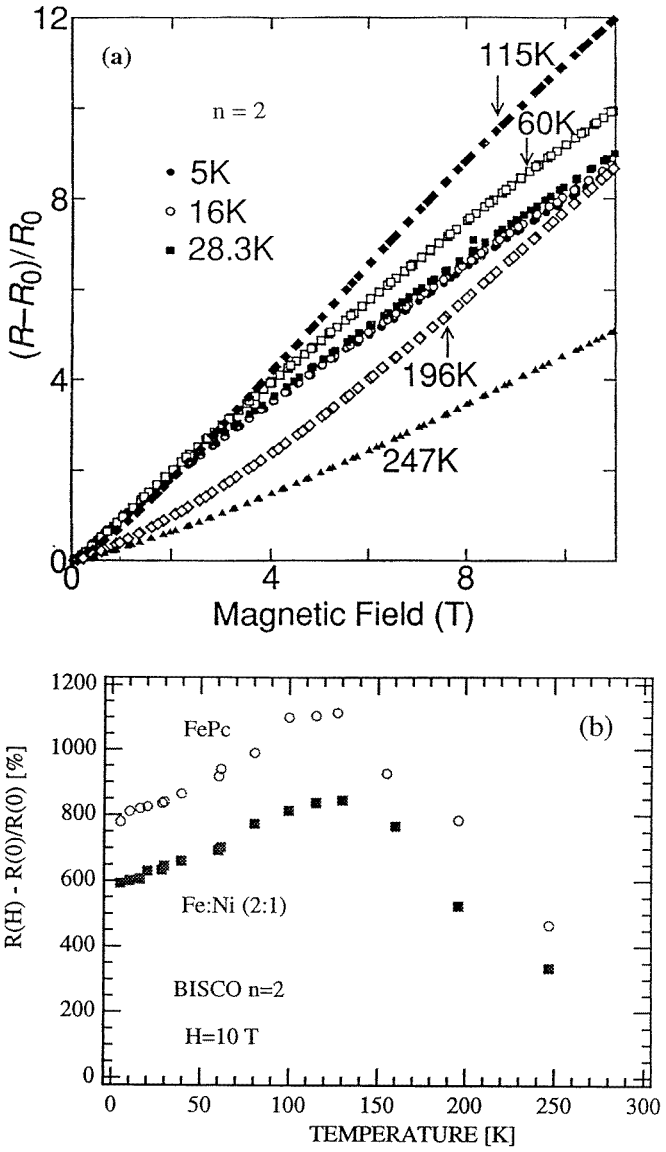

Figure 7. (a) MR against applied field in the FePc-intercalated BiSCCO $n = 2$ sample at various temperatures. (b) Temperature dependence of MT (%) at 10 T in the FePc- and the mixed-metal $Ni_{1/3}Fe_{2/3}Pc$-intercalated BiSCCO $n = 2$ sample.

either CuPc, H_2Pc or PbPc were used as an intercalant, independent of host oxide.

The physical mechanism responsible for the observed anomalous large MR in the intercalated Cu oxides is not clear at present. In spite of some similarities to Mn oxides, such as crystal structure and correlation between the magnetic transition and MR, there are significant differences between our system and CMR materials. The most obvious differences are that no metal-to-insulator transition accompanying the magnetic transition is observed in our samples, and that the signs of MR are opposite. Therefore, the physical mechanism in our case is apparently not the same as in the case of CMR.

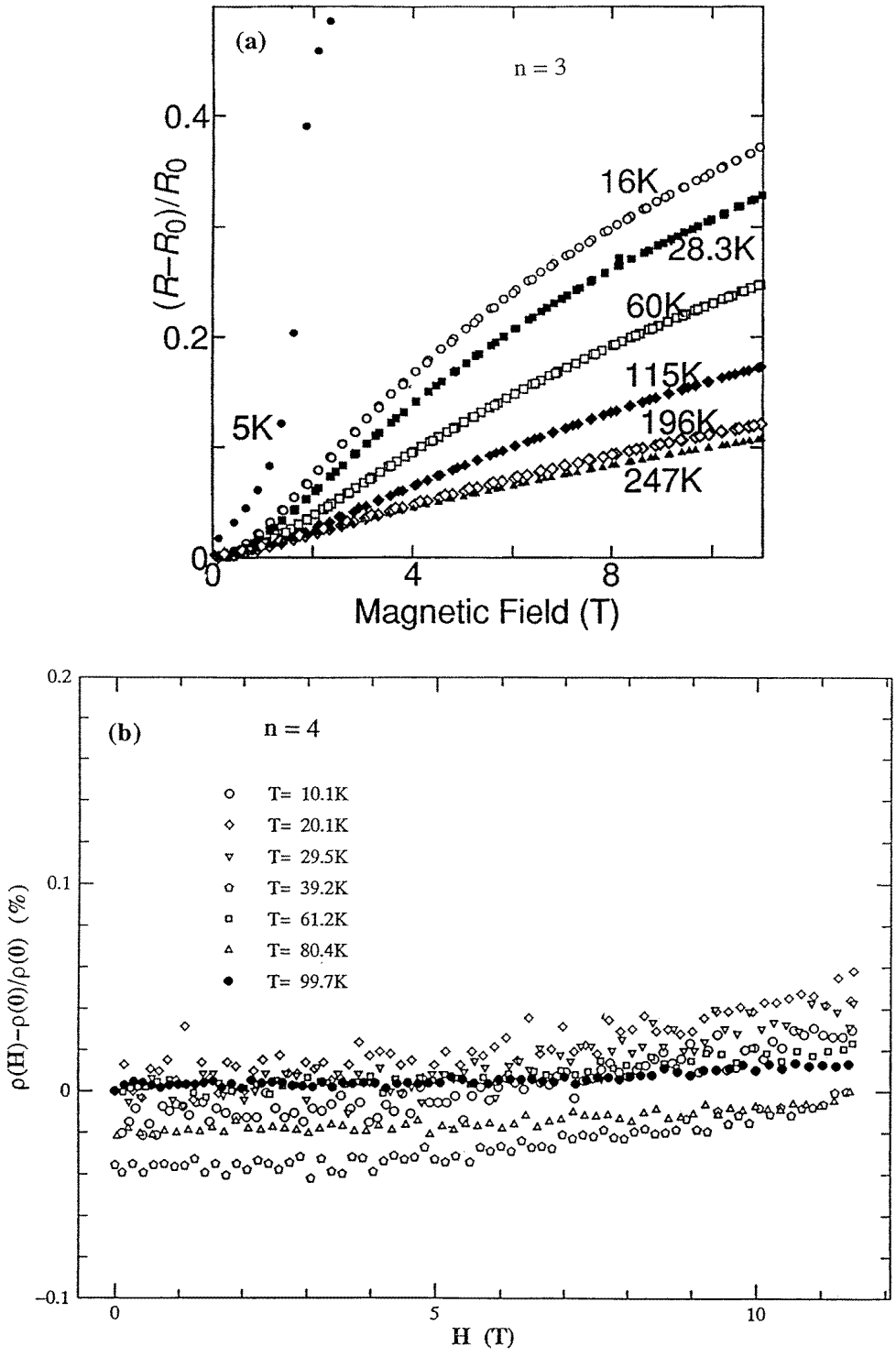

Figure 8. (a) MR in the FePc-intercalated BiSCCO $n = 3$ sample. (b) MR (%) in the FePc-intercalated BiSCCO $n = 4$ sample.

One possible scenario is related to a competition between the resonant spin-fluctuation and the spin-glass-like states, and application of an external magnetic field acts to shift the balance between the two, thereby affecting the resistance. When one of the above mechanisms clearly dominates, as spin-fluctuations do in the case of NiPc-intercalated BiSCCO $n = 2$ samples, then the effect of a magnetic field is weaker, and the values of MR are decreased. Apparently, the most delicate balance is established in the case of FePc-intercalculated BiSCO $n = 2$ samples, and that is why the resistance is strongly dependent on the applied magnetic field. One can speculate that relative contributions of the competing states are determined by interactions between the transition metal 3d orbitals of the intercalated MPc moleculars and conduction electrons of the host oxide. These interactions can be expected to depend on several important material-related factors. The first factor is a particular electronic configuration of the 3d orbitals. For example, the Ni^{2+} ions in the NiPc-intercalated BiSCCO $n = 2$ system were shown to be in a high-spin, $s = 1$ state with two unpaired spins occupying both the $3d_{z^2}$ and the $3d_{x^2-y^2}$ orbitals [4], while in the case of CuPc, there is only one unpaired spin, $s = 1/2$, and it is localized in the $3d_{x^2-y^2}$ orbital. Also important factors are the concentration of conduction electrons in the host Cu oxide, as well as relative positions and orthogonality of the Fermi level and the 3d orbitals.

To further explore and optimize LMR in the intercalated Cu oxide system, other potentially promising host materials, such as BiSCCO $n = 1$, or magnetic-metal- (such as Ni-, Co- or Mn-) based oxides, could be intercalated with MPc and tested for LMR. Another factor that seems interesting to be explored is a central metal in MPc. So far, the FePc proved to be the best choice, but other candidates such as Mn, Co, 4d and 5d transition metal MPcs and their combinations may be interesting.

In summary, an anomalous large MR or over 1200% has been observed in the intercalated Cu oxides. We relate the possible mechanism responsible for the observed LMR to a competition between the resonant spin-fluctuation and the spin-glass-like states formed in the intercalated Cu oxides. We believe that this work may open up a novel avenue to creating LMR materials.

Acknowledgments

LG acknowledges support from AIST (Japan) and DOE (USA).

References

[1] Prinz G A 1995 *Phys. Today* April 58
[2] Xiang X-D, McKernan S, Vareka W A , Zettl A, Corkill J L, Barbee T W and Cohen M L 1990 *Nature* **348** 145
[3] Pooke D, Kishio K, Koga T, Fukuda Y, Sanada N, Nagoshi M, Kitazawa K and Yamafuji K 1992 *Physica* C **198** 349
[4] Grigoryan L, Yakushi K, Narlikar A V, Dutta P K and Samantha S B 1993 *Int. J. Mod. Phys.* B **8** 615
[5] Grigoryan L, Yakushi K, Liu C-J, Takano S, Wakata M and Yamauchi H 1993 *Physica* C **218** 153
[6] Sathaiah S, Sony R N, Joshi H C, Grigoryan L, Bist H D, Narlikar A V, Samantha S B and Awana V P S 1994 *Physica* C **221** 177
[7] Grigoryan L, Chakravarty N and Capri A Z 1992 *Mod. Phys. Lett.* **6** 1843
[8] Rossiter P L 1987 *The Electrical Resisitivity of Metals and Alloys* (Cambridge: Cambridge University Press)
[9] Rivier N and Zlatic V 1972 *J. Phys. F: Met. Phys.* **2** L87
[10] Anderson P W 1961 *Phys. Rev.* **124** 41
[11] Wolff P A 1961 *Phys. Rev.* **124** 1030
[12] Rivier N and Zlatic V 1972 *J. Phys. F: Met. Phys.* **2** L99
[13] Rivier N and Zitkova J 1971 *Adv. Phys.* **20** 143

[14] Fisher K H 1974 *J. Low Temp. Phys.* **17** 87
[15] Berkovitz A E, Mitchell J M, Carey M J, Young A P, Hang S Z, Parker F T and Thomas G 1992 *Phys. Rev. Lett.* **68** 3744
[16] Schad R, Potter C D, Belien P, Verbanck G, Moshchalkov V V and Bruynseraede Y 1994 *Appl. Phys. Lett.* **64** 3500
[17] McCormack M, Jin S, Tiefel T H, Fleming R M, Philips J M and Ramesh R 1994 *Appl. Phys. Lett.* **64** 3045
[18] Gupta A, McGuire T R, Duncombe P R, Rupp M, Sun J Z, Gallagher W J and Xiao Gang 1995 *Appl. Phys. Lett.* **67** 3494
[19] Ju H L, Kwon C, Li Qi, Greene R L and Venkatesan T 1994 *Appl. Phys. Lett.* **65** 2108
[20] Hwang H Y, Cheong S-W, Radaelli P G, Marezio M and Batlogg B 1995 *Phys. Rev. Lett.* **75** 914